Eur. Phys. J. Plus (2021) 136:1177
https://doi.org/10.1140/epjp/s13360-021-02179-0

THE EUROPEAN PHYSICAL JOURNAL PLUS

Regular Article

CF-LIBS study of pure Ta, and WTa + D coating as fusion-relevant materials: a step towards future in situ compositional quantification at atmospheric pressure

Vishal Dwivedi[1], **Matej Veis**[1,2], **Alicia Marín Roldán**[1], **Eduard Grigore**[3], **Flaviu Baiasu**[3], **Iva Bogdanovič Radovič**[4], **Zdravko Siketić**[4], **Pavel Veis**[1,a]

[1] Department of Experimental Physics, FMPI, Comenius University, Mlynská dol. F2, 842 48 Bratislava, Slovakia
[2] Department of Inorganic Chemistry, FNS, Comenius University, Ilkovičova 6, Bratislava 842 15, Slovakia
[3] NILPRP 409, 077125 Magurele, Bucharest, Romania
[4] Department of Experimental Physics, Ruder Boskovic Institute, Bijenicka 54, 10000 Zagreb, Croatia

Received: 1 April 2021 / Accepted: 10 November 2021

Abstract Tungsten (W) and its alloys are being considered as a major candidate for the plasma-facing components (PFCs) in future fusion devices. Being versatile and able to perform *in situ* measurements, laser-induced breakdown spectroscopy (LIBS) is the most promising analytical tool for the elemental characterization of fusion-relevant materials. The present article studies the use of calibration free (CF)-LIBS for the characterization of the plasma generated from tantalum (Ta) and elemental quantification of WTa (5 at.%) + Deuterium (D) (10 at.%) sample (coating thickness ~ 3 μm) on molybdenum (Mo) substrate, using a high energy Nd:YAG laser (1064 nm, pulse duration 8 ns). The laser energy has been optimized (58 mJ/pulse) for given samples, and the laser-induced plasma was generated on the surface by means of focussing the laser. All the experimental measurements have been performed in air at atmospheric pressure and room temperature. For the quantification of WTa + D coating, measurements have also been performed under the flow of nitrogen gas. For the detection of the analytes, both gate delay (t_d) and gate width (t_g) were optimized. For the CF quantification, it has been found that the most appropriate gate times were $t_d = t_g = 1$ μs, considering thermodynamic equilibrium. Suitable emission from both neutral and ionic species has been considered for the evaluation of the plasma temperature and electron density using the Boltzmann and Saha–Boltzmann plots approaches, respectively. This work provides a step towards CF-LIBS quantification and depth profile analysis studies for WTa-based materials and D retention in it. These results have been compared with those obtained by other analytical techniques (TOF-ERDA and GDOES).

1 Introduction

A fusion reaction is a potential source of safe, non-carbon emitting, and abundant energy [1]. Research and developments have been done to harness fusion power and building future

[a] e-mail: veis@fmph.uniba.sk (corresponding author)

Published online: 24 November 2021

fusion power plants (ITER and DEMO). Such kind of machines consists of a great number of components. For the smooth functionality and achieving its goal, the choice of suitable materials and monitoring their behaviour under different possible conditions have prime importance.

Considering its high melting point, high thermal conductivity, low erosion, low sputtering ratio, low hydrogen (H) permeability, and strong mechanical properties, tungsten (W) and its alloys are being considered as major candidates for the first wall and divertor material in future fusion devices [2–4]. Studies have shown that under fusion favourable conditions (up to 1300 K operating temperature, 1–20 MWm^{-2} heat flux, 14 MeV neutron, and up to 3.5 MeV He^{+} ion bombardment), properties and morphology of W and W-based materials could be changed [5, 6]. Alloying W, with other transition and refractory metals like tantalum (Ta) (high-Z = 73), could be a possible way to overcome this issue. Although Ta is rare and it is difficult to use it for bulk application on large fusion devices, WTa alloy can be a potential candidate for plasma-facing components (PFCs). However, due to the high melting temperature, the preparation of these alloys is complicated. It is worth noticing that WTa alloy has a decreased fragility, better performance under thermal shock loading, and no significant increase in the fuel retention than pure W [7, 8]. Several analytical techniques such as thermal desorption spectroscopy (TDS), atom probe tomography (APT), X-ray fluorescence analysis (XRF), scanning electron microscopy (SEM), and X-ray diffraction analysis (XRD) have been applied for the characterization of W, Ta, and WTa coatings [8–10]. There are few studies on different aspects of laser interaction with Ta and related alloys. There are some, but very few studies related to the application of CF-LIBS for WTa coating [11–16].

Laser-induced breakdown spectroscopy (LIBS) technique is a well-established approach for the qualitative and quantitative elemental analysis and depth profile analysis of almost any kind of sample. It has a wide range of applications, including fusion research [17–19]. Under stoichiometric ablation and local thermodynamic equilibrium (LTE) conditions, laser-generated plasma provides information related to the composition and the characteristics of the sample [20, 21]. Owing to its in situ measurement capability, LIBS has been proposed as a promising candidate in fusion research. To obtain detailed information and develop a methodology for the characterization and depth profile quantification of fusion-relevant materials, studies related to different kinds of materials such as beryllium (Be)-based coatings, molybdenum (Mo), lithium (Li)-based coatings, and W- Copper (Cu) alloys using calibration-free (CF) LIBS approach have been done, in recent research works [22–28].

CF-LIBS provides information about the elemental composition of a sample using the plasma parameters, electron temperature (T_e) and electron density (n_e) [29]. Also, the selection of suitable spectral lines from different degrees of ionization plays a vital role in the determination of the plasma parameters. The two main goals of the current work are the following: i) to use a laser-induced plasma of pure Ta for the precise plasma parameters characterization and preselection of suitable Ta lines (interference-free from W lines), and ii) an overall quantification of WTa + D coating from the average depth and space CF-LIBS measurements as a first step towards future CF-LIBS depth profile elemental analysis of fuel (D) retention in WTa-based mixed layers. The Boltzmann plot (BP) method has been used for the evaluation of T_e, and Saha–Boltzmann (SB) plot approach has been used for the evaluation of n_e, in the present work [30]. These results have been compared with those obtained by other analytical techniques: time-of-flight elastic recoil detection analysis (TOF-ERDA) and glow discharge optical emission spectroscopy (GDOES), finding a good agreement.

2 Materials and methods

2.1 Samples

The main focus of the study is the analysis of WTa (5 at.%) + D (10 at.%) coating (coating thickness ~ 3 μm) on a Mo substrate. Additionally, measurements of isolated W and Ta samples were included for benchmarking purposes. W metal was obtained from TESLA — producer of electronic tubes, Ta was extracted from a capacitor. Quantitative purity of the metals is not precisely known; nonetheless, identification of important lines was possible. WTa + D coating sample was prepared at NILPRP, Romania, by using a dual magnetron sputtering system [31, 32]. The magnetron targets, made of W, respectively, Ta, were independently powered. This fact allowed to presume sufficient stoichiometry of the coating.

3 Experimental set-up

The experimental set-up used for the LIBS measurements is similar to our previous work [23]. Figure 1 represents a schematic diagram of the used experimental set-up. For laser ablation, a Q-switched Nd:YAG pulsed laser (Big sky laser, Quantel, 1064 nm, pulse duration 8 ns, max. energy 400 mJ/pulse) has been focussed on the surface of the sample (installed on a XYZ translational stage) using a bi-convex lens (Thorlabs, UV-fused silica, focal length 10 cm). A polarizer has been used to adjust the energy of the laser beam prior reaching the focussing lens. The laser fluence was adjusted to be closed to the threshold of the laser ablation process. The laser energy in pulse was measured using digital optical power and energy metre (Thorlabs, PM100D). Emission from the plasma has been collected using a quartz optical fibre (Thorlabs, dia. 1000 μm, 0.5 NA) aligned at 45^0 collection geometry, and fed to the echelle spectrograph (ME5000, Andor technology, 200 nm–975 nm, aperture F/7, resolution 4000) coupled with an ICCD camera (istar DH734, Andor technology). The spectrometer was triggered automatically by the laser and controlled by a personal computer (PC).

3.1 LIBS measurements

After calibrating the spectrometer for wavelength, using a mercury–argon (Hg-Ar) light source/lamp (Ocean Optics), LIBS spectra were recorded at atmospheric pressure in ambient

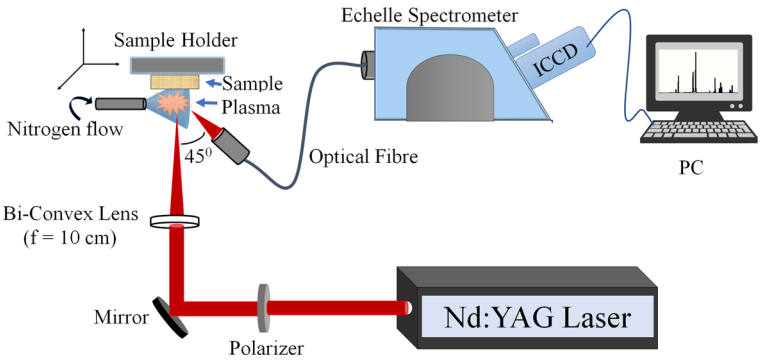

Fig. 1 Schematic diagram of LIBS experimental set-up

air and under nitrogen (N_2) flow resp., for all three samples. Considering the importance of the gate delay (t_d) and gate width (t_g) in CF-LIBS analysis, these parameters were optimized carefully for the samples used in the study.

In our work, firstly, the pure Ta LIBS spectra have been measured at atmospheric pressure in ambient air with different delay and gate times (e.g. $t_d = t_g = 150$ ns, 200 ns, 300 ns, 400 ns, 600 ns, 1 μs, 1.5 μs, and 2 μs) for the estimation of plasma parameters (T_e and n_e) and to obtain a general idea about suitable conditions for the measurement of WTa + D coating. After getting an optimized value of t_d and t_g, pure W sample has been measured only for the $t_d = t_g = 1$ μs, to get an idea about W spectral lines. For W and Ta, 50 accumulated consequent laser shots were recorded from four different spots on the sample surface. Thus, each spectrum consists of 200 accumulated laser shots, providing an improved signal to noise ratio (single shot spectrum 41.8 to accumulated spectrum 138.1). The values of delay and gate times $t_d = t_g = 500$ ns and 1 μs were found more appropriate for CF-LIBS measurements of mixed WTa + D coating. For the analysis of this coating, firstly, the kinetic series (a series of 50 consecutive laser shots at the same spot) of 50 laser shots per spot (four different spots) has been measured in order to observe an estimation of the ablation rate and depth profile, both under ambient air and N_2 flow (Linde gas, purity 5.0). Laser fluence has been kept to 58 mJ/pulse throughout the measurements (lowest laser energy possible with our set-up). This low fluence value allows us to obtain a better depth resolution and lower ablation rate. Consequently, only those spectra from kinetic series originated from the coating were chosen for the accumulated spectrum for further CF-LIBS average layer elemental analysis, including the D quantification for future fuel retention analysis.

4 Results

4.1 Spectral analysis of pure Ta and W samples, and WTa + D coating

Figure 2 shows an example of the spectra of the pure W and Ta samples (measured in ambient air) and the WTa + D coating (measured both in ambient air and under N_2 flow), at 9 different spectral ranges 300.2–302 nm, 309.8–310.7 nm, 331.5–332.7 nm, 333–334.2 nm, 481–482.2 nm, 500–502 nm, 564–565.5 nm, 630–631.3 nm, and 648–649 nm, representing spectral emission of Ta I-II and W I-II lines. Spectra for pure W and Ta samples were obtained by accumulating 50 laser shots at the same position in four different spots, and for coating (WTa + D/Mo), summarized first 20 shots from the kinetic series of 50 from 10 different spots on the surface of the sample have been considered to improve the signal to noise ratio and so the reproducibility. Globally, each spectrum consists of 200 accumulated laser shots giving us the resulting coating LIBS spectra averaged in both depth and space.

The assignation of each spectral line has been done comparing the experimental spectra with our simulated spectra calculated using NIST atomic line and Kurucz databases [33, 34]. A careful selection of suitable spectral lines for the construction of Boltzmann and SB plots was performed, choosing interference-free, non-self-absorbed lines with sufficiently high Einstein coefficients ($A > 10^6$ s^{-1}) for W, and ($A > 5 \cdot 10^5$ s^{-1}) for Ta as the number of suitable lines was slightly limited [35, 36].

4.2 Characterization of pure Ta sample using LIBS

Figure 3 shows an example of (a) the BP and (b) SB plot of the selected lines of Ta I-II, for the delay time 1 μs.

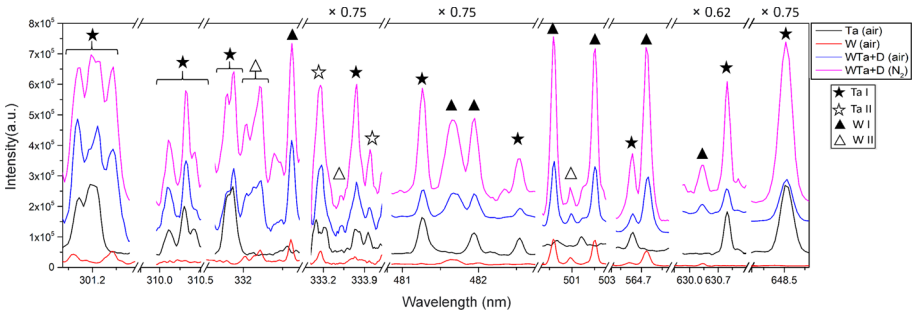

Fig. 2 Example of the emission LIBS spectra of the pure W and Ta, and the WTa + D coating at $t_d = t_g =$ 1 μs

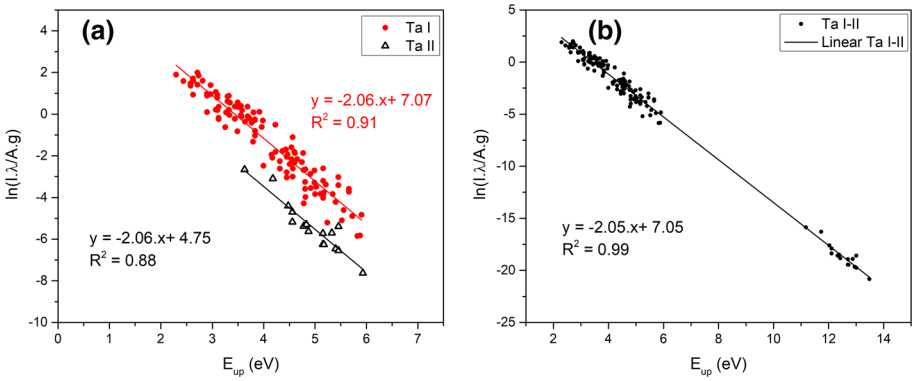

Fig. 3 **a** BP for Ta I and Ta II spectral lines **b** SB plot for Ta I-II (measured under ambient air at $t_d = t_g =$ 1 μs)

Assuming that the plasma is optically thin (selected self-absorption free lines) and in local thermodynamic equilibrium, the plasma temperature (T_e) can be found from the slope of the BP as [29]:

$$ln\frac{I \cdot \lambda}{g \cdot A} = -\frac{1}{T \cdot k_B} \cdot E_k + ln\frac{C \cdot F}{U(T)}$$

where I is the intensity (sensitivity corrected) of a spectral line (in our case calculated as the integrated area under the peak), A is Einstein's coefficient of the corresponding transition, g is the statistical weight, E_k is the energy of the upper state, T is the temperature, k_B is the Boltzmann constant, C is the concentration, F is an experimental parameter, and U (T) is the partition function.

Plasma temperature has been evaluated from the BP of neutral and singly ionized Ta lines. Numeric values, obtained from both degree of ionization, were found in a good agreement. Electron density has been evaluated using the Saha equation considering the electron temperature as an average value of the T_e obtained from the BPs for neutral and ionic species. The results of plasma parameters T_e and n_e are summarized in Table 1 and Fig. 4.

Table 1 shows the T_e and n_e values in laser-produced plasma plumes evaluated for delay and gate times ranging from 150 ns to 2 μs. The obtained results validate the assumption of LTE and satisfy the McWhirter criterion [21], for all the studied delays, taking the max-

Table 1 The obtained values of T_e and n_e for different delay and gate times

Gate delay	T_e (eV)			n_e (cm^{-3})
	BP Ta I	BP Ta II	Avg. Ta I-II	SB Ta I-II
150 ns	0.80 ± 0.08	0.76 ± 0.10	0.78 ± 0.09	$5.7 \cdot 10^{17} \pm 1.5 \cdot 10^{17}$
200 ns	0.74 ± 0.07	0.72 ± 0.11	0.73 ± 0.09	$2.6 \cdot 10^{17} \pm 7.7 \cdot 10^{16}$
300 ns	0.64 ± 0.08	0.61 ± 0.11	0.62 ± 0.09	$1.1 \cdot 10^{17} \pm 5.2 \cdot 10^{16}$
400 ns	0.58 ± 0.07	0.54 ± 0.12	0.56 ± 0.10	$1.6 \cdot 10^{16} \pm 5.2 \cdot 10^{15}$
600 ns	0.50 ± 0.07	0.50 ± 0.17	0.50 ± 0.12	$7.2 \cdot 10^{15} \pm 4.1 \cdot 10^{15}$
1 μs	0.49 ± 0.06	0.48 ± 0.20	0.49 ± 0.13	$3.6 \cdot 10^{15} \pm 1.7 \cdot 10^{15}$
1.5 μs	0.46 ± 0.07	–	0.46 ± 0.07	$3.4 \cdot 10^{15} \pm 2.1 \cdot 10^{15}$
2 μs	0.46 ± 0.10	–	0.46 ± 0.10	$1.3 \cdot 10^{15} \pm 9.8 \cdot 10^{14}$

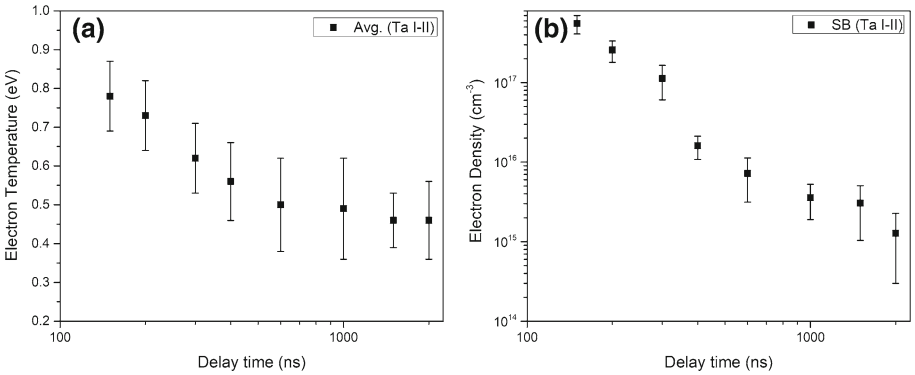

Fig. 4 Temporal evolution of the **a** T_e and **b** n_e

imal difference of energy levels corresponding to D_α line at 656 nm for future planned D quantification analysis.

Figure 4 shows the a) T_e and b) n_e in the laser-produced plasma plumes as a function of the delay time. The error bars along the y-axis show the variation of the T_e and n_e. The values have been obtained from the SB plot. As it is expected, the plasma cools down and expands when increasing the delay time.

4.3 Depth profile analysis and quantification of WTa + D coating

Elemental LIBS depth profiles were extracted using persistent and representative neutral lines. Examples of such profiles for the WTa + D coating sample, measured under N_2 flow at the delay time of 1 μs, are shown in Fig. 5. The WTa + D coating sample was prepared by sputtering in a gas environment (under deuterium discharge afterglow atmosphere) which resulted in them being quite porous, unlike samples prepared in vacuum. As the sample was exposed to air (including humidity) during transportation and storage, we assume that atmospheric gasses were trapped inside the pores to some degree. Moreover, our measurements were performed under a N_2 flow which prevents us from quantifying the N content. Thus, we deliberately choose not to include spectral lines from N, O, H and other small impurities

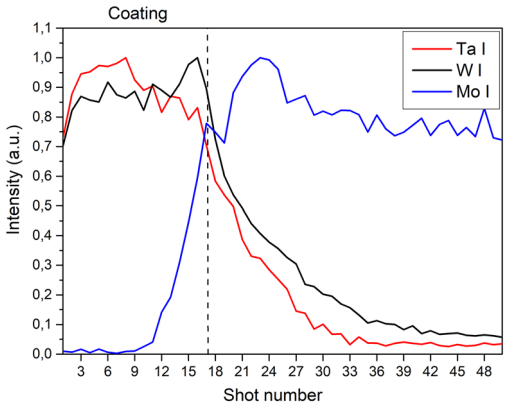

Fig. 5 LIBS depth profiles of different elements (W, Ta, Mo) in the WTa + D/Mo sample measured under N_2 atmosphere at $t_d = t_g = 1$ μs

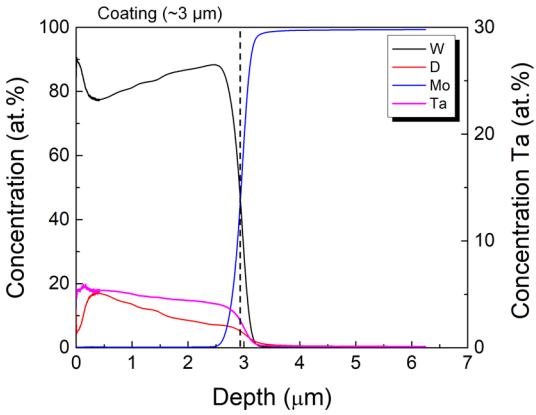

Fig. 6 GDOES depth profile of the sample WTa + D, showing the thickness of coating (~3 μm)

(though observed), and quantified the relative concentration of elements that we did consider, i.e. W, Ta, D for the three analytical techniques under study.

As it can be observed in Fig. 5, the Mo spectral lines belonging to the substrate start to appear at the laser pulse number 17 in the LIBS profiles. The spectral lines applied for the depth profile are W I 501.5 nm, 505.3 nm, 573.5 nm; Ta I 481.2 nm, 630.9 nm, 648.5 nm; Mo I 550.6 nm, 553.3 nm. The ablation rate was found ~ 176 nm/shot.

Elemental GDOES depth profiles have been obtained using a Spectruma Analytik GmbH equipment. The equipment is provided with a monochromator that was set at the wavelength of 656.078 nm corresponding to the D emission line. The resolution of the spectrometer is 25 pm, and consequently, the D line can be separated from the H line situated at 656.28 nm.

As it can be observed from Fig. 6, the GDOES depth profile indicates a relatively uniform Ta distribution across the coating, with a Ta concentration of ~ 4.65 at.%. As far as D depth profile is concerned, we observe a distribution in the range 15.3–6.8 at.% (an average value of 10 at.%). The thickness of the coatings, as it was revealed by GDOES, is ~ 3 μm.

Figure 7 shows the BPs of both W I-II and Ta I-II species from the LIBS spectrum of WTa + D coating measured at two distinct atmospheres: air (Fig. 6a and c) and N_2 flow (Fig. 6b and d) with both delay and gate time equal to 1 μs. The database values for the spectral lines used in the BPs were taken from NIST atomic line and Kurucz databases [33, 34]. The T_e evaluation of the WTa + D spectra from the surface material was performed for two distinct

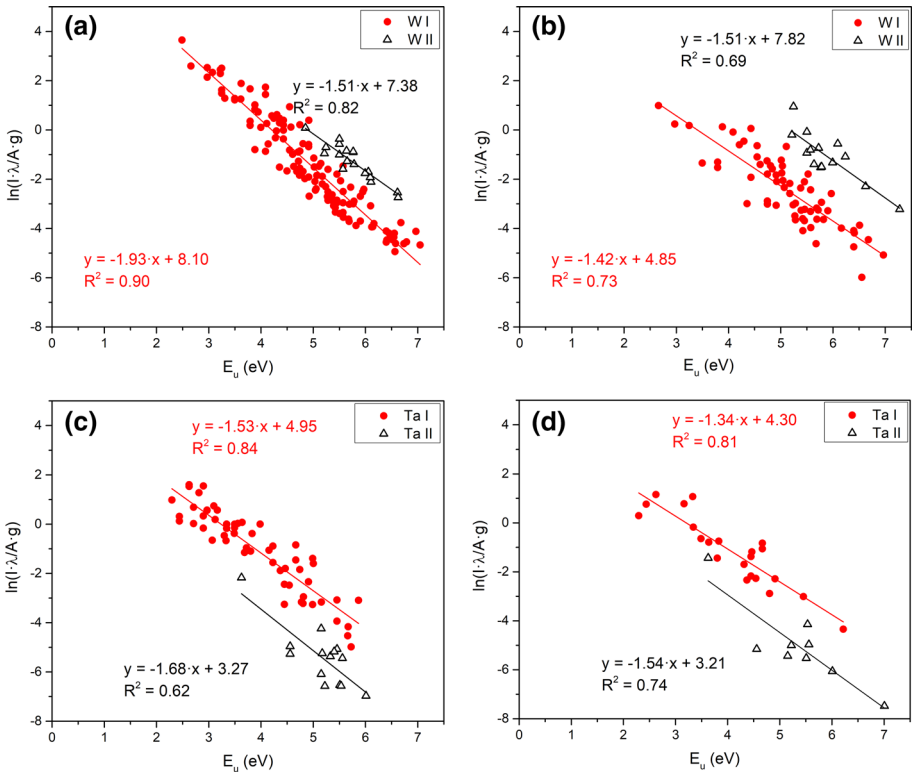

Fig. 7 BP of the WTa + D coating measured at $t_d = t_g = 1$ µs under air (a and c) and under N_2 (b and d) at atmospheric pressure

Table 2 The obtained values of T_e (eV) from the WTa + D sample

Exp. cond *Elements*	500 ns (air)	1 µs (air)	500 ns (N_2)	1 µs (N_2)
Ta I	0.81 ± 0.07	0.65 ± 0.09	0.72 ± 0.14	0.75 ± 0.13
Ta II	0.70 ± 0.13	0.60 ± 0.14	0.70 ± 0.37	0.65 ± 0.31
W I	0.58 ± 0.05	0.52 ± 0.05	0.78 ± 0.12	0.70 ± 0.11
W II	0.86 ± 0.15	0.66 ± 0.16	0.69 ± 0.42	0.66 ± 0.28

delay/gate times 500 ns and 1 µs (always equal) for both atmospheres (ambient air and N_2 flow). The obtained values are shown in Table 2.

For the electron density evaluation, the method based on the Stark broadening of D_α and H_α at 656 nm could not be used because this doublet was just partially resolved and overlapped with weak Ta I lines at 656.16 nm and 656.42 nm, and weak W I lines at 656.32 nm (see Fig. 8). Therefore, the evaluation of their broadening parameters by means of fitting profiles was unfeasible. However, the evaluation of their intensities was possible.

After the evaluation of the T_e, the CF-LIBS approach allows us to quantify W and Ta in the sample without the necessity of calibration references [29]. Values for the partition function of the used elements have been calculated using the literature Irwin 1981 [37]. These

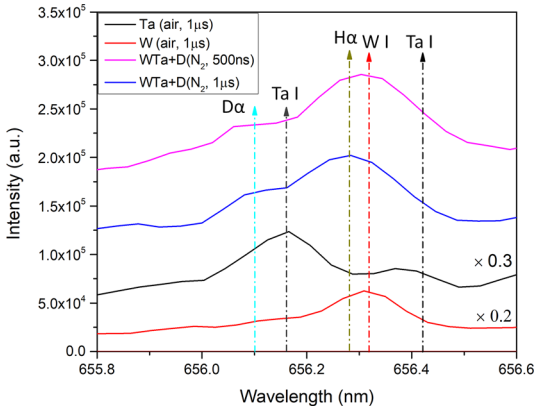

Fig. 8 Overlapping of D_α at 656.1 nm, Ta I at 656.16 nm H_α at 656.28 nm, W I at 656.32 nm and Ta I at 656.42 nm

Table 3 Elemental composition of the sample WTa + D

Exp. cond *Elements*	500 ns (air) (without D)	1 μs (air) (without D)	500 ns (N_2) (without D)	1 μs (N_2) (without D)	1 μs (N_2) (with D)	TOF-ERDA (with D)*	GDOES (with D)**
D [at.%]	–	–	–	–	21.5	12.3	10
Ta [at.%]	10.1	5.2	12.6	5.6	4.2	87.7	4.6
W [at.%]	89.9	94.8	87.4	94.4	74.3		85.4

*It should be noticed that only first ~ $1000 \cdot 10^{15}$ at./cm2 of sample was analysed which corresponds to about 200–250 nm

**The D content is obtained for the distribution in the coating in the range of 15.3–6.8 at.% (an average value of 10 at.%), and the Ta content is in the range 4.1–5.2 at.% (an average value ~ 4.6 at.%)

analyses were performed for 500 ns and 1 μs delays in both ambient air atmosphere and N_2 flow.

The results are presented in Table 3. In the first four columns, we can clearly see that the results from CF-LIBS quantitative analysis are closer to the nominal production ratio of WTa coating sample (95:5) at higher delays (1 μs) in both air and N_2 flow conditions. These are more probable due to the fact that at the beginning (500 ns), the slight differences between the T_e from different elements and different degrees of ionisation can still be observed. At the highest delay, the $n_e$is smaller, giving narrower spectral lines and consequently, more precise integration of the spectral lines in the LIBS spectra, as dense as those of W and Ta are. TOF-ERDA measurements were done using in house-built spectrometer [38]. For the measurement, 23 MeV $^{127}I^{7+}$ beam (beam profile at the sample is around 2×3 mm^2) obtained from the EN Tandem accelerator at the Ruder Boskovic Institute in Zagreb was used. Spectrometer was placed at 37.5°, and angle between sample surface and beam was 20°. A comparison among CF-LIBS, TOF-ERDA, and GDOES results is presented in Table 3.

For the quantification of D in the studied WTa + D sample by CF-LIBS, it is important to know whether the LTE conditions are also valid for H. (The McWhirter criterion [21] was fulfilled for all four studied conditions of delays and atmospheres and also for the highest difference of energy levels of D_α at 656 nm.) From Table 2, it can be concluded that all T_e

values are very similar, confirming also the LTE condition. But, the T_e obtained from neutral Boltzmann plots was more precise as the T_e obtained from the ionic Boltzmann plots as the higher number of point in the Boltzmann plot make the T_e evaluation more precise (see Fig. 6). For the quantification, we have used each individual T_e for each corresponding element and degree of ionization, except for D, that we use the Ta I T_e value. Two consecutive steps for the evaluation of D content were performed. The first one consists on using a Gaussian fitting for all the overlapping spectral lines from the partially resolved line at around 656 nm: D_α (656.1 nm), Ta I (656.16 nm), H_α (656.28 nm), W I (656.32 nm), and Ta I (656.42 nm), considering a different FWHM for D_α and H_α from the rest of lines. Finally, only the area belonging to D_α and Ta, subtracting the rest of the lines from the experimental spectral line, was taken into account in the next step.

The second step for D quantification was a numerical simulation, based on the subtraction of the surface of the Ta I spectral line at 656.16 nm from the first partially resolved peak, calculating the area of Ta line using the Boltzmann equation and known spectral parameters. This area value was after the subtraction from the total area of the partially resolved line at 656 nm. All necessary parameters were taken from the NIST database [33], and these lines have also been verified in the BPs of pure Ta and W from the previous LIBS analysis. After subtraction of the interfering Ta line, we could precisely quantify the WTa + D elemental composition, including D (see Table 3, column 5). This analysis was done at the conditions closest to those desired by ITER (at atmospheric pressure of an inert atmosphere without Oxygen—no air) [39]. The approximate uncertainty level for CF-LIBS is ~ 20%, while particularly for D, the error goes up to 50% due to the limitations of the single pulse LIBS analysis for H isotopes.

5 Conclusions

This study investigates the use of LIBS for the characterization of pure Ta, W, and WTa + D coating as well as the CF-LIBS quantification of WTa + D coating material. LIBS allows for a straightforward depth profile analysis which has been performed on the WTa + D coating. It has shown the presence of W, Ta, and Mo (from the substrate); moreover, from the depth of the coating, the ablation rate (~ 176 nm/shot) has been determined. A careful preselection of suitable Ta and W lines, (self-absorption free, interference-free lines, and not too weak intensity and transition probability), and the plasma parameters (temperature and electron density) evaluation were performed for the pure Ta sample by using the BPs and the Saha equation. The quantitative analysis for the composition of the WTa + D coating sample has been performed by CF-LIBS by averaging the whole depth in ten different positions from the analysis on the coating. We have found that the results from CF-LIBS are closer to the nominal production ratio of WTa coating sample (95:5) at higher delays (1 μs) in both air and N_2 flow conditions. The average value of deuterium in the coating was in the order of 20 at.%. We consider this work, realized at atmospheric pressure under N_2 flow, as the first step for future CF-LIBS depth profile elemental analysis of fuel (D) retention in WTa-based mixed layers, using rapid, *in situ*, and remote-friendly method. The quantitative results obtained by CF-LIBS are in good agreement with those obtained by other analytical techniques (TOF-ERDA and GDOES).

Acknowledgements We would like to acknowledge the Scientific Grant Agency of the Slovak Republic (contract number VEGA-1/0803/21, VEGA-2/0144/21) and SRDA (APVV-16-0612) for financial support. This work has been carried out within the framework of the EUROfusion Consortium and has received funding

from the Euratom research and training programme 2014−2018 and 2019−2020 Under Grant Agreement No. 633053. The views and opinions expressed herein do not necessarily reflect those of the European Commission.

Declarations

Conflict of interest The authors declare that they have no conflict of interest.

CRediT author statement: Vishal Dwivedi was involved in investigation, visualization, formal analysis, writing—original draft. **Matej Veis** contributed to formal analysis, software, writing—review and editing. **Alicia Marín Roldán** was involved in visualization, writing—review and editing. **Eduard Grigore and Flaviu Baiasu** contributed to resources, investigation**,** visualization, formal analysis. **Iva Bogdanović Radović** and **Zdravko Siketić** were involved in resources, investigation, formal analysis. **Pavel Veis contributed to** conceptualization, formal analysis, resources, investigation, writing—review and editing, supervision.

References

1. Culham Centre for Fusion Energy (https://ccfe.ukaea.uk/whyfusion.aspx) (n.d.)
2. N. Baluc, Plasma Phys. Control. Fusion **48**, B165 (2006)
3. M.J. Rubel, G. Sergienko, A. Kreter, A. Pospieszczyk, M. Psoda, E. Wessel, Fusion Eng. Des. **83**, 1049 (2008)
4. M. Rieth, S.L. Dudarev, S.M. Gonzalez de Vicente, J. Aktaa, T. Ahlgren, S. Antusch, D.E.J. Armstrong, M. Balden, N. Baluc, M.-F. Barthe, W.W. Basuki, M. Battabyal, C.S. Becquart, D. Blagoeva, H. Boldyryeva, J. Brinkmann, M. Celino, L. Ciupinski, J.B. Correia, A. De Backer, C. Domain, E. Gaganidze, C. García-Rosales, J. Gibson, M.R. Gilbert, S. Giusepponi, B. Gludovatz, H. Greuner, K. Heinola, T. Höschen, A. Hoffmann, N. Holstein, F. Koch, W. Krauss, H. Li, S. Lindig, J. Linke, Ch. Linsmeier, P. López-Ruiz, H. Maier, J. Matejicek, T.P. Mishra, M. Muhammed, A. Muñoz, M. Muzyk, K. Nordlund, D. Nguyen-Manh, J. Opschoor, N. Ordás, T. Palacios, G. Pintsuk, R. Pippan, J. Reiser, J. Riesch, S.G. Roberts, L. Romaner, M. Rosiński, M. Sanchez, W. Schulmeyer, H. Traxler, A. Ureña, J.G. van der Laan, L. Veleva, S. Wahlberg, M. Walter, T. Weber, T. Weitkamp, S. Wurster, M.A. Yar, J.H. You, A. Zivelonghi, J. Nucl. Mater. **432**, 482 (2013)
5. M. Seo, J.R. Echols, A.L. Winfrey, Npj Materials Degradation **4**, 1 (2020)
6. E. Bernard, R. Sakamoto, A. Kreter, M.F. Barthe, E. Autissier, P. Desgardin, H. Yamada, S. Garcia-Argote, G. Pieters, J. Chêne, B. Rousseau, C. Grisolia, Phys. Scr. **T170**, 014023 (2017)
7. V.I. Dubinko, P. Grigorev, A. Bakaev, D. Terentyev, G. van Oost, F. Gao, D. Van Neck, E.E. Zhurkin, J Phys Condens Matter **26**, 395001 (2014)
8. V. M. Lunyov, A. S. Kuprin, V. D. Ovcharenko, V. A. Belous, A. N. Morozov, A. V. Ilchenko, G. N. Tolmachova, E. N. Reshetnyak, and R. L. Vasilenko, Voprosy Atomnoj Nauki i Tekhniki 140 (2016)
9. Y. Zayachuk, M. H. J. \textquotesinglet Hoen, P. A. Z. van Emmichoven, I. Uytdenhouwen, and G. van Oost, Nucl. Fusion **52**, 103021(2012)
10. A. Xu, D.E.J. Armstrong, C. Beck, M.P. Moody, G.D.W. Smith, P.A.J. Bagot, S.G. Roberts, Acta Mater. **124**, 71 (2017)
11. E.V. Struleva, P.S. Komarov, S.I. Ashitkov, High Temp **56**, 648 (2018)
12. L. Torrisi, F. Caridi, A. Picciotto, D. Margarone, A. Borrielli, J. Appl. Phys. **100**, 093306 (2006)
13. S. Khan, S. Bashir, A. Hayat, M. Khaleeq-ur-Rahman, and Faizan–ul-Haq, Physics of Plasmas **20**, 073104 (2013)
14. S. Mittelmann, J. Oelmann, S. Brezinsek, D. Wu, H. Ding, G. Pretzler, Appl. Phys. A **126**, 672 (2020)
15. K. Ibano, D. Nishijima, Y. Ueda, R.P. Doerner, J. Nucl. Mater. **522**, 324 (2019)
16. C. Li, J. You, H. Wu, D. Wu, L. Sun, J. Liu, Q. Li, R. Hai, X. Wu, H. Ding, Plasma Sci. Technol. **22**, 074008 (2020)
17. G.S. Maurya, A. Marín-Roldán, P. Veis, A.K. Pathak, P. Sen, J. Nucl. Mater. **541**, 152417 (2020)
18. C. Li, C.-L. Feng, H.Y. Oderji, G.-N. Luo, H.-B. Ding, Front. Phys. **11**, 114214 (2016)
19. V. Philipps, A. Malaquias, A. Hakola, J. Karhunen, G. Maddaluno, S. Almaviva, L. Caneve, F. Colao, E. Fortuna, P. Gasior, M. Kubkowska, A. Czarnecka, M. Laan, A. Lissovski, P. Paris, H.J. van der Meiden, P. Petersson, M. Rubel, A. Huber, M. Zlobinski, B. Schweer, N. Gierse, Q. Xiao, G. Sergienko, Nucl. Fusion **53**, 093002 (2013)

20. J.A. Aguilera, C. Aragón, V. Madurga, J. Manrique, Spectrochim. Acta, Part B **64**, 993 (2009)
21. G. Cristoforetti, A. De Giacomo, M. Dell'Aglio, S. Legnaioli, E. Tognoni, V. Palleschi, N. Omenetto, Spectrochim. Acta, Part B **65**, 86 (2010)
22. P. Veis, A. Marín-Roldán, V. Dwivedi, J. Karhunen, P. Paris, I. Jõgi, C. Porosnicu, C.P. Lungu, V. Nemanic, A. Hakola, Phys. Scr. **T171**, 014073 (2020)
23. A. Marín Roldán, M. Pisarčík, M. Veis, M. Držík, and P. Veis, Spectrochimica Acta Part B: Atomic Spectroscopy **177**, 106055 (2021)
24. P. Veis, S. Atikkuke, A. Marin Roldan, V. Dwivedi, M. Veis, P. Barton, M. Jerab, R. Dejarnac, Nuclear Materials and Energy **25**, 100809 (2020)
25. L. Mercadier, A. Semerok, P.A. Kizub, A.V. Leontyev, J. Hermann, C. Grisolia, P.-Y. Thro, J. Nucl. Mater. **414**, 485 (2011)
26. M. Kubkowska, P. Gasior, M. Rosinski, J. Wolowski, M.J. Sadowski, K. Malinowski, E. Skladnik-Sadowska, Eur. Phys. J. D **54**, 463 (2009)
27. I. Jõgi, P. Paris, M. Laan, J. Kozlova, H. Mändar, M. Passoni, D. Dellasega, A. Hakola, H.J. van der Meiden, J. Nucl. Mater. **544**, 152660 (2021)
28. V. Dwivedi, A. Marín Roldán, J. Karhunen, P. Paris, I. Jõgi, C. Porosnicu, C. P. Lungu, H. J. van der Meiden, A. Hakola, P. Veis, Nuclear Materials and Energy **27**, 100990 (2021)
29. A. Ciucci, M. Corsi, V. Palleschi, S. Rastelli, A. Salvetti, E. Tognoni, Appl Spectrosc **53**, 960 (1999)
30. V.K. Unnikrishnan, K. Alti, V.B. Kartha, C. Santhosh, G.P. Gupta, B.M. Suri, Pramana - J Phys **74**, 983 (2010)
31. J. Musil, P. Baroch, IEEE Trans. Plasma Sci. **33**, 338 (2005)
32. A. Aijaz, D. Lundin, P. Larsson, U. Helmersson, Surf. Coat. Technol. **204**, 2165 (2010)
33. A. Kramida, Yu. Ralchenko, J. Reader, and NIST ASD Team, (2020)
34. P. L. Smith, Atomic spectral line database from CD-ROM 23 of R. L. Kurucz, (n.d.)
35. A. De Giacomo, Spectrochim. Acta, Part B **58**, 71 (2003)
36. Q. Abbass, N. Ahmed, R. Ahmed, M.A. Baig, Plasma Chem Plasma Process **36**, 1287 (2016)
37. A.W. Irwin, Astrophys. J. Suppl. Ser. **45**, 621 (1981)
38. Z. Siketić, N. Skukan, and I. Bogdanović Radović, Review of Scientific Instruments **86**, 083301 (2015)
39. H. van der Meiden, S. Almaviva, G. Maddaluno, J. Butikova, V. Dwivedi, A. Marín Roldán, M. Veis, P. Veis, P. Gasior, W. Gromelski, M. Kubkowska, A. Hakola, X. Jiang, G. Sergienko, S. Brezinsek, I. Jogi, P. Paris, K. Piip, and J. Karhunen, Nuclear Fusion **61**, 125001 (2021). https://doi.org/10.1088/1741-4326/ac31d6